OPTIMIZING REINFORCEMENT LAYOUT IN CONCRETE DESIGN CONSIDERING CONSTRUCTABILITY

Yang Yang, PhD Candidate, Johns Hopkins University, Baltimore, MD
James K. Guest, PhD, Johns Hopkins University, Baltimore, MD
Cristopher D. Moen, PhD, P.E., Virginia Tech, Blacksburg, VA

ABSTRACT

Structural topology optimization is increasingly being used to remove the guesswork in identifying natural force flow paths for reinforced concrete and prestressed concrete, particularly for complex 3D design domains. Tension and compressive forces that follow the principle stress trajectories, i.e., ties and struts, are automatically identified with topology optimization using a formulation that minimizes strain energy, or equivalently that minimize crack widths. While a useful alternative to trial-and-error process of generating strut-and-tie models (STM), the approach falls short of design objectives as it neglects constructability and rebar detailing, which is often the governing cost. This paper uses a new advancement in topology optimization for addressing constructability issues by considering both material and construction costs. By assigning different construction costs for each tension tie (rebar or prestressing), the placement of steel can be controlled to a large extent by the designer, thus it is capable of generating practical designs that also perform well in service. A hybrid truss-continuum FE model with bilinear orthotropic material properties is used to generate the optimized strut-and-tie models that can be used directly for design and detailing. Results demonstrate that the designer gains the ability to explore tradeoffs between material and labor cost while maintaining reinforcement layouts that ensure structural integrity at service and ultimate limit states.

Keywords: Structural optimization, Topology optimization, Strut-and-tie model, Reinforced concrete, Prestressed concrete, Construction cost

INTRODUCTION

It is common practice in structural concrete design to divide structural components into two regions, one where stress can be computed from elastic bending theory, often referred as B-regions, and the other where the strain distribution is significantly nonlinear (e.g., near concentrated loads, supports, openings, etc.) known as discontinuous-regions, or D-regions. A common approach to designing B-regions under shear is to assume the flow of forces can be represented as a truss. This truss analogy, first proposed by Ritter [1], assumes that the cracked concrete structure acts as a truss with top and bottom longitudinal chords and an inclined web at 45 degrees. Mörsch [2] later suggested the use of diagonals different from 45 degrees and introduced the use of this truss model for torsion. D-regions, on the other hand, have been designed using rules of thumb or past experience for many years. The landmark paper by Jörg Schlaich and his colleagues at the University of Stuttgart (Schlaich et al. [3]) proposed generalizing the truss analogy to apply it in the form of strut-and-tie-models (STM) to all parts of the structure including both B-regions and D-regions. STM is a generalized truss model that consists concrete compression struts, steel tension ties, and nodal zones. It has been introduced into many design specifications and widely used in practical design for the past two decades.

STMs are also particularly suitable for the design of anchorage zones of prestressed concrete structures. It deals with the design of the transverse reinforcement that resists the tensile force induced by prestressed tendons. Since each prestressing tendon and support reaction is modeled as a concentrated load at the beam end, the anchorage zone is highly discontinuous when the number of prestressing tendons is large and/or the support reaction cannot be neglected. For these cases, the use of STMs is of great importance.

Generating an effective STM becomes more challenging when the geometry of the problem becomes complicated, such as beams with cutouts, or the applied load and boundary conditions leads to complicated stress states. Additionally there are, theoretically, an infinite number of STM possibilities for a given problem. Navigating these possibilities with a trial-and-error approach can dramatically increase design time and costs. Topology optimization, on the other hand, is an automated design process where an optimization algorithm is used to distribute material (struts and ties) through the concrete domain. Design specifications are posed as constraints that the optimizer must not violate.

Topology optimization is gaining momentum in the structural engineering community, with several firms using it to generate concepts for tall buildings (e.g., Baker et al. [4]; Sarkisian et al. [5]).Several works have considered using topology optimization to design STM (Kumar [6], Ali [7], Biondini et al. [8, 9], Ali and White [10], Moen and Guest [11,] Kim and Baker [12,], Guan [13], Liang [14,], Nagarajan and Madhavan Pillai [15], Bruggi [16,]). An example from Moen and Guest [11], given in Fig. 1, is used to illustrate how truss topology optimization can be used to visualize force paths and to develop strut-and-tie models. The STM, based on the traditional method, is developed for a reinforced concrete deep beam in Fig. 1a and superposed over experimental results from Nagarajan and Pillai [17]. The steel reinforcement is orthogonal to cracks at midspan, but loses efficiency near the supports where cracks are diagonal. Fig. 1b shows an alternative STM developed by minimum compliance topology optimization method. The optimizer here places steel orthogonal to the compression struts, creating a steel reinforcement layout that orthogonally bridges cracks (indicated in the background experimental images), thereby increasing flexural capacity.

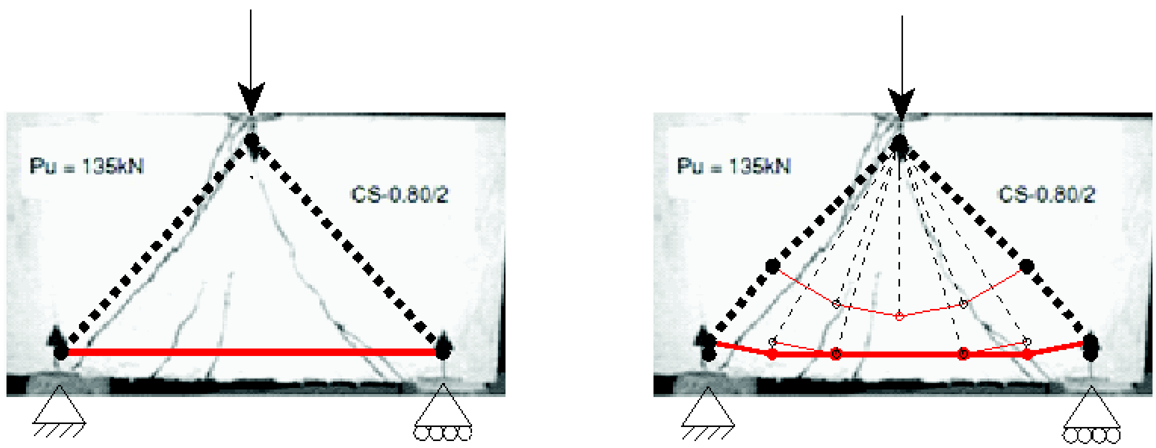

(a) Traditional design (b) Minimum compliance design

Fig. 1. Compare (a) traditional STM and (b) minimum compliance STM derived with topology optimization. Black dashed lines represent compression carried by the concrete, red solid lines represent tension carried by the reinforcing steel. Experimental results provided in the background are taken from Nagarajan and Pillai [17].

More recently, hybrid truss-continuum approaches have been explored, where the continuum represents compression load paths and the truss elements represent straight steel members, which are more reasonable representations of steel rebar and more easily constructed. This idea was put forth at a recent Structures Congress (Guest and Moen [18]), and achieved in Gaynor et al. [19], Yang et al. [20] and Yang et al. [21] using bilinear stress-dependent material models for the truss and continuum domains, described in 2D and 3D, respectively. Amir and Sigmund [22] likewise used a truss-continuum approach, but utilized elastoplastic model to differentiate between the tension and compression load paths.

Although design complexity can be controlled through selection of the truss ground structure according to these papers, placement cost of reinforcing steel has not been investigated. The presence of inclined reinforcing steel, for example, may increase labor costs and perhaps total costs of a system, over a simpler design of horizontal bars that is less efficient and thus uses more steel. Thus, considering construction cost is crucial to make the optimized results practical. Recently, Asadpoure et al. [23] addressed a similar problem in the design of truss structures by adding a per-element unit cost to the material cost function. This cost was meant to represent the cost of placing a truss member into the structural system and the labor cost of making two connections. The approach is adapted here to the hybrid topology optimization approach and used to penalize, through cost, complex reinforcing patterns.

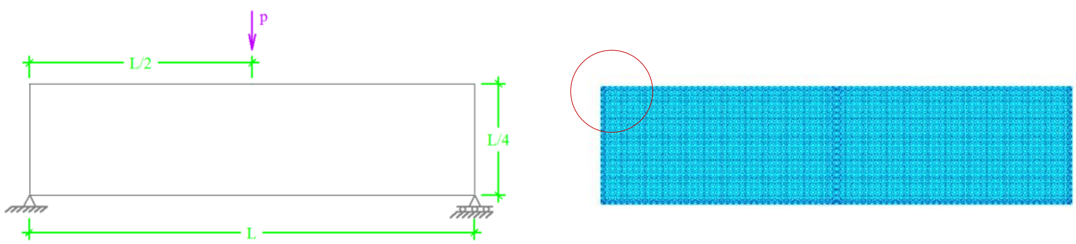

(a) Design Domain (b) Hybrid Discretization

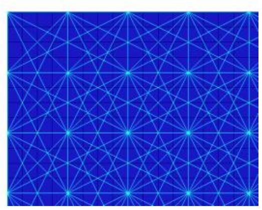

(c) Detail of Hybrid Discretization (b)

Fig. 2. Design domain and hybrid discretization for topology optimization of simply supported beam

TOPOLOGY OPTIMIZATION FORMULATION CONSIDERING MATERIAL AND CONSTRUCTION COSTS

The first step of topology optimization process is to express the design problem formally as an optimization problem. In this paper, a minimum compliance, or equivalently maximum stiffness, topology optimization framework is adopted. This formulation minimizes external work, or equivalently internal strain energy, leading to the design of structures where forces follow the stiffest load path.

The topology optimization process then continues by meshing the design domain, which in the hybrid truss-continuum approach consists of a truss ground structure representing the steel embedded in a continuum finite element discretization representing the concrete (Figure 2). The goal of the optimizer is then to determine the cross-sectional area $\boldsymbol{\rho}_\mathbf{t}$ of the truss elements and the volume fraction $\boldsymbol{\rho}_\mathbf{c}$ of the continuum elements, where $\boldsymbol{\rho}_\mathbf{c} = 1$ indicates compression-carrying concrete and $\boldsymbol{\rho}_\mathbf{c} = 0$ indicates non-load carrying concrete. Truss elements with non-zero cross-sectional area then represent the steel reinforcement design (the ties) and continuum elements with $\boldsymbol{\rho}_\mathbf{c} = 1$ representing the compression load path (the struts).

Let us express the external work as $\mathbf{F}^T\mathbf{u}$, where $\mathbf{F}$ are the applied nodal loads and $\mathbf{u}$ the nodal displacements, with equilibrium as $\mathbf{Ku} = \mathbf{F}$, where K is the global stiffness matrix, which we note is a function of the design variables ρ_t and ρ_c. The minimum compliance (maximum stiffness) optimization problem can then be stated as:

$$
\begin{aligned}
\min_{\boldsymbol{\rho}_\mathbf{c},\, \boldsymbol{\rho}_\mathbf{t}} \quad & f(\boldsymbol{\rho}_\mathbf{c}, \boldsymbol{\rho}_\mathbf{t}) = \mathbf{F}^T\mathbf{u} \\
s.t. \quad & \mathbf{K}(\boldsymbol{\rho}_\mathbf{c}, \boldsymbol{\rho}_\mathbf{t}, \boldsymbol{\sigma}_\mathbf{c}, \boldsymbol{\sigma}_\mathbf{t})\mathbf{u} = \mathbf{F} \\
& M(\rho_c^e, \rho_t^e) + C(\rho_t^e) \le TC \\
& 0 < \rho_{\min} \le \rho_c^e \le 1, \ \forall e \in \Omega_c \\
& 0 \le \rho_t^e, \ \forall e \in \Omega_t
\end{aligned}
\tag{1}
$$

where the second constraint is the total cost TC constraint, composed of the material cost M and construction cost C; the third set of constraints are the design variable bounds on the continuum elements in the domain (denoted as Ω_c), with ρ_{min} selected as a small positive number to maintain positive definiteness of the global stiffness matrix; and the fourth set of constraints are the design variables bounds on the truss elements in the domain (denoted as Ω_t).

In the total cost constraint, the material cost is computed as

$$
M(r_c^e, r_t^e) = \sum_{e \in W_c} a_c^e r_c^e v_c^e + \sum_{e \in W_t} a_s^e r_t^e v_t^e
\tag{2}
$$

where v_c^e denotes the element volume for continuum concrete, v_t^e the length for steel bars, and α_c^e and α_t^e represent material cost per unit volume for concrete and steel, respectively. These terms typically appear in minimum compliance problem as a material volume usage constraint. The construction cost, recently proposed in Asadpoure et al. [23] to represent fabrication cost in discrete structures, is computed as

$$C(\rho_t^e) = \sum_{e\in\Omega_t} \alpha_f^e H^e(\rho_t^e) \tag{3}$$

Where the function H represents the Heaviside step function such that any truss element with cross-sectonal area greater than zero counts as an element that must be constructed, or placed. Note that only the truss (steel) elements appear in this function as the continuum elements represent the concrete domain. The variable α_f^e denotes the construction cost of placing the element e. In truss structures, for example, it represented the labor cost of member placement (including crane time) and making two connections, one at each end of the member. The magnitude of the element construction cost is ultimately dictated by the local market and construction methods, but our goal herein is to show how the magnitude of this cost term can be used to influence the constructability of rebar schedules.

As the step function H is discrete, it must be regularized for use with gradient-based optimizers. We use the regularization function discussed in Asadpoure et al. [23], originally proposed by Guest et al. [24] for projection methods in continuum topology optimization, given as follows:

$$H^e(\rho_t^e) = 1 - e^{-\beta(\rho_t^e)} + (\rho_t^e)e^{-\beta} \tag{4}$$

Where β is regularization parameter that dictates how aggressively the step function approximated (Guest et al. [25]), set to 10 in this paper. Note that using this expression, if a steel truss member achieves a non-zero cross-sectional area, this function yields a magnitude of one, which imposes the element's unit cost on the total cost function.

It is seen that when $\alpha_c^e = \alpha_s^e$ and $\alpha_f^e = 0$, this total cost constraint is equivalent to the simple volume constraint used in Yang et al. [20]. For the sake of comparing the material and construction costs and showing the effect of the latter on simplifying the optimized placement of reinforcing steel, α_c^e and α_s^e are set fixed and equal to unit. Thus changing the value of α_f^e will change the ratio of construction and material cost. We want to emphasize that the values of these parameters can be determined based on actual cost of concrete and steel, and local labor costs of placing steel bars.

The Heaviside Projection Method (HPM) (Guest et al. [24], Guest [26]) is used to avoid well-known numerical instabilities of checkerboards and mesh dependency associated with continuum elements. Sensitivities are calculated using the adjoint method (see Gaynor et al. [19] for equations corresponding to the hybrid topology optimization) and the gradient-based optimizer is chosen as the Method of Moving Asymptotes (MMA) (Svanberg [27]), which is very efficient for structural optimization. Full algorithmic details for this approach are available in Guest et al. [25].

Finally, we note that underlying the hybrid truss-continuum approach is a bilinear, stress-dependent mechanics model that is formulated such that the truss (steel) elements carry only tension and the continuum (concrete) elements carry only compression. The details of this model were presented at the 2013 **PCI** Convention and **National Bridge Conference** (Yang et al. [20]), and briefly summarized in the Appendix for convenience. The numerical examples in this paper assume Young's modulus for the concrete is 24.9 GPa (3600 ksi) in compression and 2.0 GPa (290 ksi) in tension, while Young's modulus for the steel is 200 GPa (29000ksi) in tension and zero in compression, to ensure compression load paths are carried by the concrete (see Appendix).

NUMERICAL EXAMPLES

The first numerical example is the benchmark simply supported beam problem loaded at midspan, as shown in Fig. 3a. A traditional STM is shown in Fig. 3b along with a topology-optimized solution considering only material cost, without construction cost, in Fig. 3c. It is well-known that minimum strain energy topologies will mimic the principal stress trajectories, and so we have enabled a fine structural topology to closely approximate this and emphasize the difference when considering constructability. Of course simpler topologies could be achieved by altering the initial ground structure (see Gaynor et al. [19] for a discussion on this). Fig. 3d displays the solution when significantly increasing the unit labor cost to unit material cost ratio. The topology clearly contains fewer bars and is a significantly simpler topology that would be easier (and cheaper) to construct. These bars, however, have significantly larger cross-sectional area, leading to a much larger total material cost than those found Fig. 3c. The solution in Fig. 3e was found by assigning a high cost to the use of inclined rebar relative to the cost of horizontal and vertical rebar. This led the algorithm to avoid using inclined rebar, despite their extreme structural efficiency for this design example. Note that two inclined bars did appear in the final topology, as the cost was not high enough to overcome their structural efficiency and corresponding material cost savings.

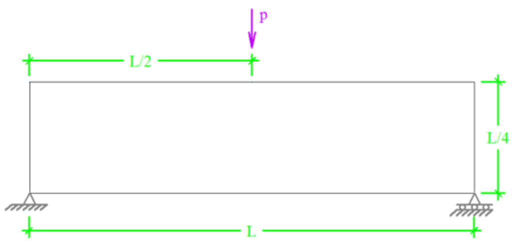

(a) Design domain

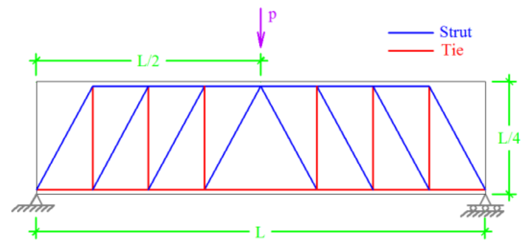

(b) A traditional STM

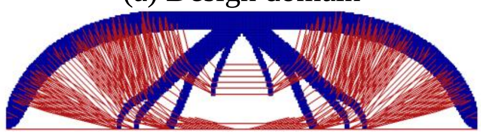

(c) Optimized STM without considering construction cost ($\alpha_c^e = \alpha_s^e = 1$, $\alpha_f^e = 0$)

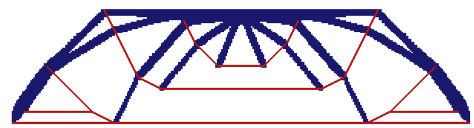

(d) Optimized STM considering construction cost ($\alpha_c^e = \alpha_s^e = 1, \alpha_f^e = 2$ for all steel reinforcement)

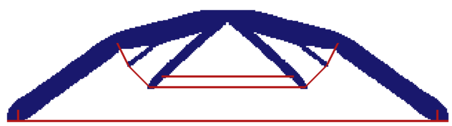

(e) Optimized STM considering construction cost ($\alpha_c^e = \alpha_s^e = 1, a_f^e = 2$ for inclined rebar, $a_f^e = 0.5$ for all others)

Fig. 3. Topology optimization of STM considering construction cost

Another benchmark example is a deep beam with cutouts as shown in Fig. 4a. A traditional STM with horizontal and vertical steel ties only is illustrated in Fig. 4b. Fig. 4c gives a topology-optimized solution considering only material cost. It has been seen that it consists of a large number of steel rebar, which makes the proposed STM less practical. In Fig. 4d, the result accounting for both material and construction costs has a much simpler STM. In Fig. 4e, a different STM which has less inclined steel reinforcement is obtained by increasing the construction cost of these steel rebar.

While these results should be considered preliminary, they show the potential of incorporating labor cost into STM optimization. Of course one of the key challenges is properly quantifying labor costs, which are highly driven by local markets. In this work, however, we simply express these costs as a ratio to material costs to illustrate the idea and explore the tradeoffs between material and constriction costs.

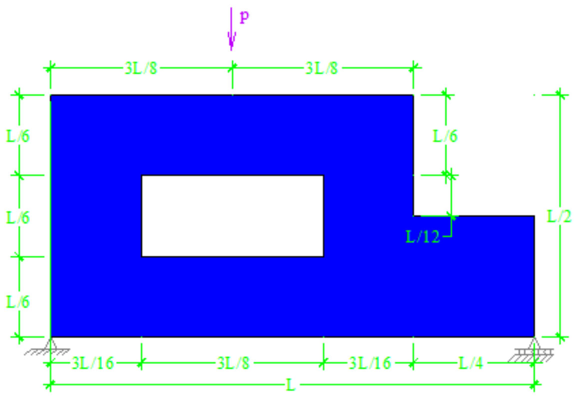

(a) Design domain

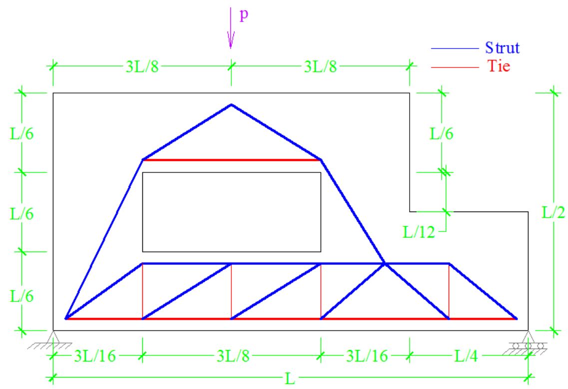

(b) A traditional STM

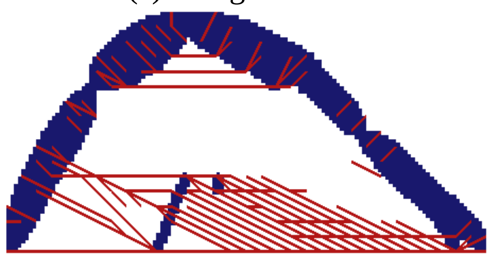

(c) Optimized STM without considering construction cost ($\alpha_c^{\ e} = \alpha_s^{\ e} = 1,\ \alpha_f^{\ e} = 0$)

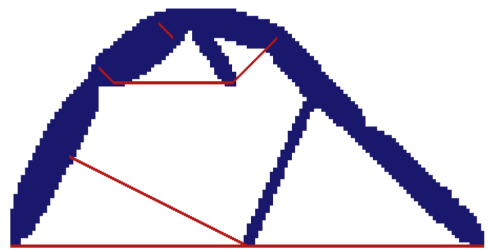

(d) Optimized STM considering construction cost ($\alpha_c^{\ e} = \alpha_s^{\ e} = 1,$ $\alpha_f^{\ e} = 2$)

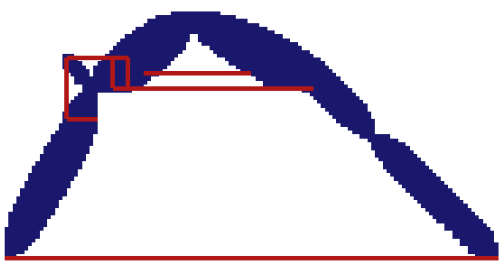

(e) Optimized STM considering construction cost ($\alpha_c^{\ e} = \alpha_s^{\ e} = 1, \alpha_f^{\ e} = 6$ for inclined rebar, $a_f^e = 0.5$ for all others)

Fig. 4. Topology optimization of STM considering construction cost

CONCLUSIONS

Topology optimization has recently been shown as an effective design tool for visualizing the flow of forces in concrete and producing efficient STM. This paper take use of a hybrid truss-continuum model, following the idea of Gaynor et al. [19] and Yang et al. [20], to focus tensile forces in the steel (truss) and compressive forces in the concrete (continuum).

While traditional topology optimization approaches consider only material cost, this paper proposes including construction cost, which is also of great importance, into the topology optimization of STM. Following the work of Asadpoure et al. [23], construction cost is estimated as a unit cost associated with placing a rebar element, with different elements potentially having different unit costs depending on their geometry and position. Although this is a simple cost model, results clearly illustrate that the complexity of STM can be influenced through this construction cost algorithm. It is the goal of future work to develop more sophisticated, more realistic construction cost models.

ACKNOWLEDGEMENTS

The authors also thank Krister Svanberg for providing the MMA optimizer code.

APPENDIX: HYBRID TRUSS-CONTINUUM STRUT-AND-TIE MODELS

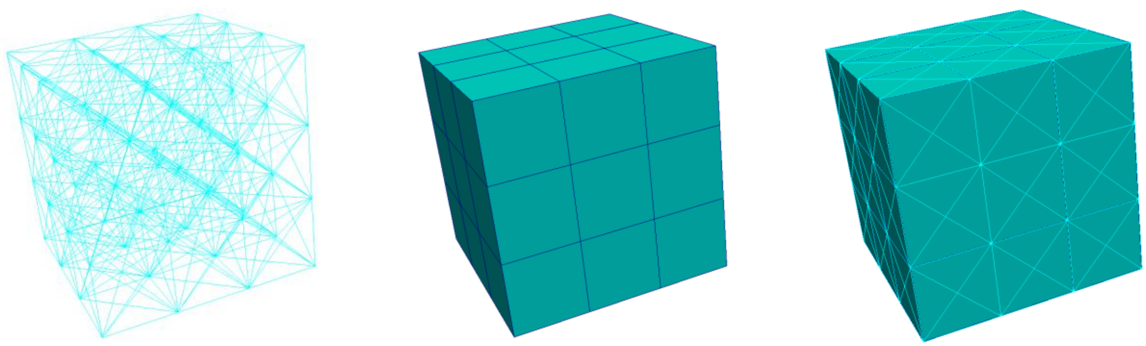

(a) Truss model (b) Continuum model (c) Hybrid truss-continuum model

Fig. 5. Hybrid mesh scheme

A typical group of elements in the hybrid truss-continuum STM developed in Yang et al. [28] is shown in Fig. 5. In this model, truss members represent steel reinforcement and continuum members are used to predict the behavior of the concrete. In order to direct tensile forces to the steel and compression forces to the concrete, the approach taken here is to use negligible compressive strength and stiffness for the steel, and negligible tensile strength and stiffness for the concrete. In order to achieve the idea that truss members only carry tensile forces, we can use a zero Young' modulus in compression, while use the actual Young' modulus of steel in tension. Continuum members can also be modeled as bimodulus materials as following; Young's modulus and Poisson's ration are E_t and υ_t, respectively, when the corresponding principal stress is in tension along certain direction; while Young's modulus and Poisson's ration are E_c and υ_c, respectively, when the corresponding principal stress is in compression along certain direction. Mathematically, the improved constitutive equation can be shown as follows [28, 29]:

$$\{\varepsilon_p\} = [a]\{\sigma_p\} = [d]^{-1}\{\sigma_p\} \tag{6}$$

where, $\{\varepsilon_p\} = \lfloor \varepsilon_{p1}, \varepsilon_{p2}, \varepsilon_{p3}, 0,0,0 \rfloor^T$ and $\{\sigma_p\} = \lfloor \sigma_{p1}, \sigma_{p2}, \sigma_{p3}, 0,0,0 \rfloor^T$ denote the stress and strain vectors in the principal stress coordinate system, respectively. The constitutive tensor can be computed corresponding to principal stresses as follows:

(a) if $\sigma_{p1} > 0, \sigma_{p2} > 0, \sigma_{p3} > 0$: $a_{ii} = \dfrac{1}{E_t}$ $(i = 1,2,3)$; $a_{ik} = -\dfrac{\upsilon_t}{E_t}$ $(i,k = 1,2,3, i \neq k)$ (7.1)

(b) if $\sigma_{p1} < 0, \sigma_{p2} < 0, \sigma_{p3} < 0$: $a_{ii} = \dfrac{1}{E_c}$ $(i = 1,2,3)$; $a_{ik} = -\dfrac{\upsilon_c}{E_c}$ $(i,k = 1,2,3, i \neq k)$ (7.2)

(c) if $\sigma_{p1} > 0, \sigma_{p2} > 0, \sigma_{p3} < 0$;

$$a_{11} = a_{22} = \frac{1}{E_t},\ a_{33} = \frac{1}{E_c},\ a_{12} = a_{21} = a_{31} = a_{32} = -\frac{\upsilon_t}{E_t},\ a_{13} = a_{23} = -\frac{\upsilon_c}{E_c} \tag{7.3}$$

(d) if $\sigma_{p1} > 0, \sigma_{p2} < 0, \sigma_{p3} < 0$;

$$a_{11} = \frac{1}{E_c},\ a_{22} = a_{33} = \frac{1}{E_t},\ a_{12} = a_{13} = a_{23} = a_{32} = -\frac{\upsilon_c}{E_c},\ a_{21} = a_{31} = -\frac{\upsilon_t}{E_t} \tag{7.4}$$

The constitutive tensor $[d]$ can be obtained by inverting the flexibility matrix $[a]$. The remaining undetermined terms d_{44}, d_{55} and d_{66} can be obtained by assuming the following

$$d_{44} = d_{55} = d_{66} = \frac{\eta E_t + (1-\eta)E_c}{2\eta(1+\upsilon_t) + 2(1-\eta)(1+\upsilon_c)} \tag{8}$$

where η is equal to the ratio of the sum of positive principal stresses and the sum of absolute value of all principal stresses, thus $0 \leq \eta \leq 1$.

REFERENCES

1. Ritter W., "Die Bauweise Hennebique," Schweizerische Bauzeitung, V. 33, No. 7, 1899, pp. 59–61.
2. Mörsch E., “Concrete-steel construction,” E. P. Goodrich, translator, McGraw-Hill, New York; 1909.
3. Schlaich J., Schaefer K., Jennewein M., "Toward a consistent design of structural concrete," *PCI Journal*, V. 32, No. 3, May-June 1987, pp. 74-150.
4. Baker W., Beghini A., Carrion J., Mazeika A., Mazurek A., “Numerical tools in structural optimization”, Proc. of the 6th International Conference on Computation of Shell and Spatial Structures, Ithaca, NY; May 2008.
5. Sarkisian M., Long E., Shook D., Doo C.S., “Optimization Tools for the Design of Structures.” Proceedings of the 2012 Structures Congress, Chicago, Illinois, ASCE, Reston, Virginia; Mar. 2012.
6. Kumar P., "Optimal force transmission in reinforced concrete deep beams," *Computers and Structures,* V. 8, No. 2, Apr. 1978, pp. 223–229.
7. Ali M.A., "Automatic generation of truss models for the optimal design of reinforced concrete structures," PhD thesis, Cornell University, 1997.
8. Biondini F., Bontempi F., Malerba P.G., "Optimal strut-and-tie models in reinforced concrete structures," *Computer Assisted Mechanics and Engineering Sciences,* V. 6, 1999, pp. 279–293
9. Biondini F., Bontempi F., Malerba P.G., "Stress path adapting strut-and-tie models in cracked and uncracked R.C. elements," *Structural Engineering and Mechanics,* V. 12, No. 6, Jan. 2001, pp. 685–698.
10. Ali M.A., White R.N., "Formulation of optimal strut-and-tie models in design of reinforced concrete structures," *ACI Special Publications*, V. 193, Aug. 2000, pp. 979–998.
11. Moen C.D., Guest J.K., "Reinforced concrete analysis and design with truss topology optimization," Third International fib Congress and Exhibition, May 2010.
12. Kim H.A., Baker G., "Topology optimisation of reinforced concrete structures," In: Computational Mechanics - New Frontiers for the New Millennium: proceedings for the 1st Asian-Pacific congress on computational mechanics, V. 2, 2001, pp. 1251–1256.
13. Guan H., "Effect of sizes and positions of web openings on strut-and-tie models of deep beams," *Advances in Structural Engineering*, V. 8, No. 1, Jan. 2005, pp. 69–84.
14. Liang Q.Q., "Performance-based optimization of structures: theory and applications," Routledge, London, 2005, pp. 134–207.
15. Nagarajan P., Madhavan Pillai T.M., "Development of strut and tie models for simply supported deep beams using topology optimization," *Songklanakarin Journal of Science & Technology*, V. 30, No. 5, Sept.-Oct. 2008, pp. 641–647.
16. Bruggi M., "Generating strut-and-tie patterns for reinforced concrete structures using topology optimization," *Computers and structures,* V. 87, Dec. 2009, pp. 1483–1495.
17. Nagarajan P., Pillai T. M. M., "Analysis and design of simply supported deep beams using strut and tie method," *Advances in Structural Engineering*, V. 11, No. 5, Oct. 2008, pp. 491-499.

18. Guest J.K., Moen C.D., "Reinforced concrete design with topology optimization," Proceedings of 2010 Analysis & Computation Specialty Conference, ASCE Structures Congress, Orlando, FL, USA, May 2010, pp. 1-10.
19. Gaynor A.T., Guest J.K., Moen C.D., "Reinforced concrete force visualization and design using bilinear truss-continuum topology optimization," *Journal of Structural Engineering*, V. 139, No. 4, Apr. 2013, pp. 607-618.
20. Yang Y., Gaynor A.T., Moen C.D., Guest J.K., "Computer-generated force flow paths for concrete design: an alternative to traditional strut-and-tie models," Proceedings of 2013 PCI Convention and National Bridge Conference, Grapevine, TX, USA, 2013, pp. 1-13.
21. Yang Y., Moen C.D., Guest J.K., "Three-dimensional force flow paths and reinforcement design in concrete via stress-dependent truss-continuum topology optimization," *Journal of Mechanical Engineering*, in review.
22. Amir O., Sigmund O., "Reinforcement layout design for concrete structures based on continuum damage and truss topology optimization," *Structural and Multidisciplinary Optimization*, V. 47, No. 2, Feb. 2013, pp. 157–174.
23. Asadpoure A., Guest J.K., Valdevit L., "Incorporating Fabrication Cost into Topology Optimization of Discrete Structures and Lattices," *Structural and Multidisciplinary Optimization*, in review.
24. Guest J.K., Prevost J.H., and Belytschko T., "Achieving minimum length scale in topology optimization using nodal design variables and projection functions," International Journal for Numerical Methods in Engineering V. 61, No. 2, July 2004, pp. 238 - 254.
25. Guest J. K., Asadpoure A., and Ha S., "Eliminating beta continuation from Heaviside projection and density filter algorithms," *Structural and Multidisciplinary Optimization*, V. 44, No. 4, Oct. 2011, pp. 443–453.
26. Guest J.K., "Topology optimization with multiple phase projection," Computer Methods in Applied Mechanics and Engineering, V. 199, No. (1-4), Dec. 2009, pp. 123-135.
27. Svanberg K., "The method of moving asymptotes—a new method for structural optimization," *International Journal for Numerical Methods in Engineering*, V. 24, Feb. 1987, pp. 359–373.
28. Ambartsumyan S. A., and Khachatryan A. A., "The different-modulus theory of elasticity," *Mekhanika Tverdogo Tela*, V. 1, No. 6, 1966, pp. 64-67.
29. Liu X.B., Meng Q.C., "On the convergence of finite element method with different extension-compression elastic modulus," *Journal of Beijing University of Aeronautics and Astronautics*, V. 28, No. 2, Oct. 2002, pp. 231-234.